Journal of Nuclear Materials 577 (2023) 154329

Contents lists available at ScienceDirect

Journal of Nuclear Materials

journal homepage: www.elsevier.com/locate/jnucmat

Physical properties of KCl-UCl_3 molten salts as potential fuels for molten salt reactors

Hyeonwoo Kim‡, Choah Kwon‡, Seongwon Ham, Juhyung Lee, Sung Joong Kim*, Sangtae Kim*

Department of Nuclear Engineering, Hanyang University, Seoul 04763, Republic of Korea

ARTICLE INFO

Article history:
Received 21 October 2022
Revised 27 December 2022
Accepted 8 February 2023
Available online 10 February 2023

KEYWORDS:
Molten salt reactors
Molecular dynamics
KCl-UCl3
Polarizable ion model
Molten salt nuclear fuel

ABSTRACT

Passive molten salt reactors are receiving a significant amount of research attention for their inherent safety. While KCl-UCl_3 exhibit high UCl_3 loading of 53 mol% at the eutectic composition, their physical properties remain largely unexplored for both forced and natural circulation. Here, we employ classical molecular dynamics simulations to calculate the physicochemical properties of KCl-UCl_3 molten salts at various temperatures and compositions. The computed density, heat capacity, and viscosity show that only viscosity exhibits temperature dependence while the others rarely change between 600 °C to 800 °C. The computed ionic structures reveal the formation of polymer-like uranium network structures at compositions above 40% UCl_3, a distinct feature of KCl-UCl_3 compared to NaCl-33%UCl_3 eutectic mixture. We rationalize that the U network structure increases the absolute viscosity, yet also provides the temperature-dependent viscosity via allotropic U^{3+}-Cl^- polyhedral coordination. The molten salts are also assessed for both forced and natural convection with the computed physicochemical properties.

Introduction

Molten salt reactors (MSR) are an emerging reactor concept for small modular reactors which employ molten salts as both nuclear fuels and coolants [1]. The reactor type exhibits inherent safety due to atmospheric pressure operation and potentially low radioactive waste generation when operated with a fast neutron spectrum [2]. MSRs exhibit a wide range of potential applications including economical hydrogen generation via high-temperature water electrolysis [3], powering electricity-generating barge [4], or electricity supply to isolated regions. As potential fuel/coolant candidates, molten chloride salts have received considerable research attention because of their high actinide and fission product solubility and hard neutron spectrum compared to fluoride salts [2]. For instance, Terrapower has been developing molten chloride fast reactors with a NaCl-UCl_3 fuel/coolant system, which targets decarbonizing electricity while achieving highly inherent safety [5].

Designing MSRs requires the detailed fluid dynamic properties of the target molten salt systems. Especially, designing passive MSRs that do not rely on pumps but natural circulation provides upgraded safety and lowered maintenance costs, yet requires detailed fluid dynamics engineering of the reactor system [6]. However, due to the high operating temperatures and radioactivity, experimentally building the database of molten salt properties has remained severely limited for various compositions and temperatures [7–9]. Alternatively, computationally assessing the physicochemical properties via classical molecular dynamics (MD) or *ab initio* molecular dynamics (AIMD) has been of active research [10,11]. Li et al. reported the fluid properties of NaCl-UCl_3 using AIMD, providing detailed analyses of the ionic coordination around U^{3+} ions. [12] On the classical molecular dynamics side, Madden et al. developed interatomic potentials named polarizable ion models (PIM) to accurately capture the polarizability among ions and notably increased the accuracy of physical property prediction without excessively involving expensive *ab initio* force calculations [13,14]. These efforts led to the computed figure of demerit (FOD) for forced turbulent convection [15].

In terms of fuel/coolant materials, few fuel candidates have been extensively studied. For example, the physical properties of LiCl–KCl–UCl_3 eutectic mixture have been reported in various reports, in part due to its applications in spent nuclear fuel reprocessing [16,17]. Xuejiao Li *et al.* studied dynamic fluctuation of the U^{3+} coordination structure such as radial distribution functions (RDF), coordination numbers, self-diffusion coefficient, or cage volume in molten LiCl-KCl mixture via AIMD [18]. NaCl-UCl_3 molten

* Corresponding author.
E-mail addresses: sungjkim@hanyang.ac.kr (S.J. Kim), sangtae@hanyang.ac.kr (S. Kim).
‡ These authors contributed equally to this work.

https://doi.org/10.1016/j.jnucmat.2023.154329

salts have recently received a significant amount of research attention as molten salt fuels, and the temperature- and composition-dependent properties such as density, heat capacity, viscosity, and diffusivity have been reported via both classical MD simulations with PIM and AIMD simulations [15,19,20]. Despite the detailed studies, the two material systems exhibit eutectic points with only approximately 30 mol% UCl_3, making it difficult to design nuclear fuels targeting a long-term fuel cycle. On the other hand, the KCl-UCl_3 materials system exhibits three eutectic points with one eutectic point possessing 53% UCl_3 composition, exhibiting potential for loading increased U content in the salt than the NaCl counterpart [21]. Yet, the physicochemical properties of liquid KCl-UCl_3 have largely been unexplored, lacking the necessary materials' properties for the reactor designs and the scientific understanding of the molten salts' structural features at high U^{3+} content.

In this work, we utilize classical MD simulations with PIM potentials to calculate the physicochemical properties of KCl-UCl_3 materials systems, including the density, heat capacity, and viscosity according to temperature and composition. The temperature dependences of the density and viscosity are analyzed in depth, and their relevance in terms of natural circulation is discussed. Also, a large composition range from 10% to 70% UCl_3 has been studied to rigorously study the effect of increasing U^{3+} ion content in the molten salts, and the following change in U^{3+} coordination is also tracked and analyzed. The heat removal performances of the fluid are analyzed by computing the FODs for both natural and forced turbulent flow.

Material and methods

Classical MD simulations were carried out by using PIM potential [22] with detailed explanation in supplementary file (S1. The PIM potential), implemented in the CP2K package [23]. Previous works [22] employed the PIM potential in simulations under molten salt conditions. The early studies [24–26] focused on description of local structures in molten salt environments by matching spectroscopic measurements, X-ray diffraction and Raman spectroscopy, to simulation results. The potentials [17,22,27] are also appropriate to predict physicochemical properties such as density, diffusion coefficient and viscosity of molten salts. We calculated the density of KCl molten salts under various temperatures to affirm the validity of the PIM potentials in our simulations by exploiting the parameters in Table S1. The calculated density of KCl molten salts at 650 °C has 1.31 g/cm3 with less than 10% errors compared to experimental results [28]. Seven compositions from 10 at% UCl_3 to 70 at% UCl_3 mixed in KCl molten salts were simulated, in the temperature ranges from 600 °C to 800 °C at 50 °C intervals. The eutectic point composition of 53 mol% UCl_3 was computed, replacing the 50 mol% compositions. The simulation cell was sized with the initial edge sides ranging between 4.0∼4.5 nm, and all modeled systems contained between 800 and 900 ions. The equilibrium properties of the liquids are simulated first by performing MD simulations in NPT ensembles for 100 ps with timestep of 1 fs. The bulk properties of density and heat capacity are obtained, along with the structural features including the radial distribution functions (RDF) and the coordination number analyses.

Based on the equilibrated structures in the NPT ensemble calculations, the simulated cell is computed once again in the NVT ensemble for 50 ps to obtain the viscosity of the molten salts. The shear viscosities of molten salts are obtained from the Green–Kubo formulation by integrating the pressure tensor autocorrelation function:

$$\eta = \frac{V}{k_B T} \int_0^\infty dt P_{\alpha\beta}(0) P_{\alpha\beta}(t)$$

Table 1
The coefficients of thermal expansion according to the composition of the chlorine-based potassium-uranium molten salt. The thermal expansion (α_T) is given in the units of 10^{-4} °C $^{-1}$.

αT\x	0.1	0.2	0.3	0.4	0.5	0.6	0.7
$(UCl3)_x$-$(KCl)_{1-x}$	3.54	3.16	2.83	3.16	3.13	2.68	1.28

where V and $P_{\alpha\beta}(t)$ represent the volume of the particle system and off-diagonal element of the stress tensor, respectively. Viscosities were calculated as the average of 60 trajectories to increase the statistical accuracy [29]. It should be noted that we tested the convergence of the viscosity under condition of larger size model system of 1823 atoms during 1000 ps for 1 run to account for the statistical accuracy as shown in Fig. S1. The stress tensor strongly correlates until 1 ps and the fluctuation lasts until 1000 ps (Fig. S1a). The accumulated fluctuations prevent from the convergence as shown in Fig. S1b, which has also been reported by several studies [30,31]. Averaging the independent 1 ps simulations better secures the statistical accuracy than performing a long-time simulation in the KCl-UCl_3 molten salt systems.

We additionally predicted the mixing enthalpy of the KCl and UCl_3 mixtures to validate the PIM potential detailed in the supplementary note (please see Supplementary Note S2. Mixing enthalpy). The mixing enthalpy derived from the molar enthalpy in Fig. S2 was fitted to the surrounding ion model [32]. The mixing enthalpy matches well with the experiment within 5.70 kJ/mol error as shown in Fig. S3 [21].

Results

Fig. 1 shows the computed fluid dynamic properties of KCl-UCl_3 in terms of UCl_3 contents and temperature. The density of the molten salt increases from 1.77 g/cm^3 to 3.44 g/cm^3, as the UCl_3 content increases from 10% to 70%, reflecting the increased U content. At the eutectic composition of 53% UCl_3, the computed density is 3.16 g/cm^3 at 600 °C, approximately 20% lower than the experimentally reported density of 3.92 g/cm^3 [7]. The computed value is approximately 4.4 times compared to the density at the working conditions of a pressurized water reactor and approximately 0.8 times compared to that of NaCl-UCl_3 at its eutectic composition [8]. The computed density decreases with increasing temperature, down to 2.96 g/cm^3 at 800 °C.

The molar volume of UCl_3 added to KCl remains approximately identical throughout all the compositions considered and increases from 141.5 Å^3 to 148.8 Å^3 as the temperature increases from 600 °C to 800 °C (Table 1). The equivalent thermal expansion coefficient of UCl_3 derived from its molar volume inside KCl is computed to be 2.37×10^{-4}/ °C, accounting for approximately 40% of the total thermal expansion coefficient at the eutectic composition. At 60 mol% UCl_3 composition, the thermal expansion coefficient of the KCl-UCl_3 mixture interestingly falls below that of UCl_3. The computed specific heat capacity decreases from 0.77 J/g °C to 0.39 J/g °C, as the UCl_3 content increases from 10% to 70% (Fig. 1b). The error bars correspond to the standard deviations of linearly interpolated enthalpy according to the temperature change. This simply reflects the increasing weight of uranium, since the molar heat capacity remains approximately identical at 33.63 J/mol K throughout all the compositions considered.

Fig. 1c shows the computed viscosity of KCl-UCl_3 molten salts. The computed viscosity of the eutectic mixture at 600 °C is 5.84 cP. The computed viscosity gets affected more significantly by temperature than density, exhibiting lower slopes on the contour lines than those in density maps. At the low UCl_3 composition of 10 at%, the viscosity of molten salt decreases by 38.78% from 1.96 cP to 1.20 cP as the temperature increases from 600 °C to 800 °C. At

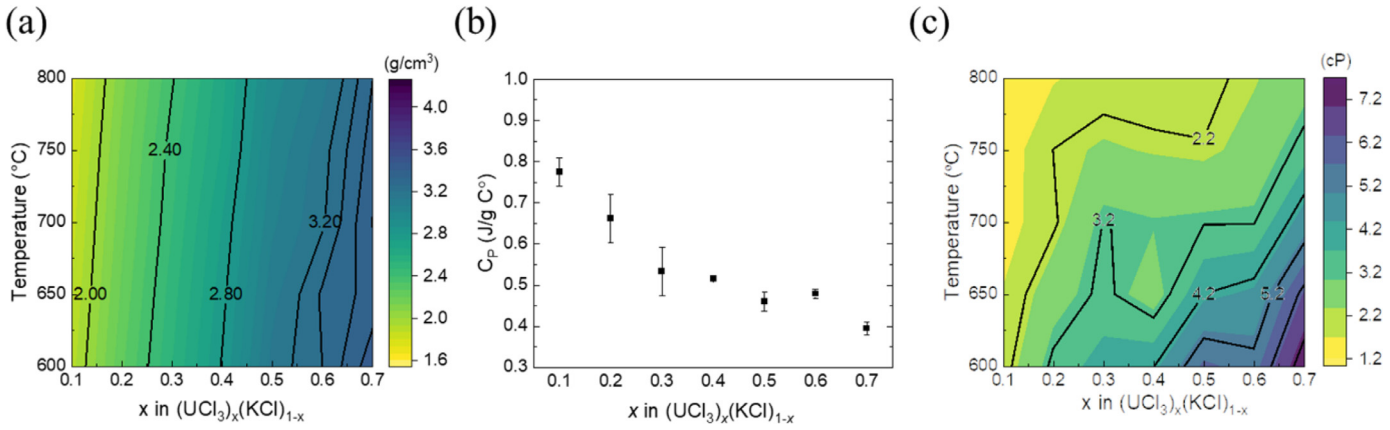

Fig. 1. The computed (a) density, (b) heat capacity and (c) viscosity of KCl-UCl3 as a function of temperature and UCl3 concentration.

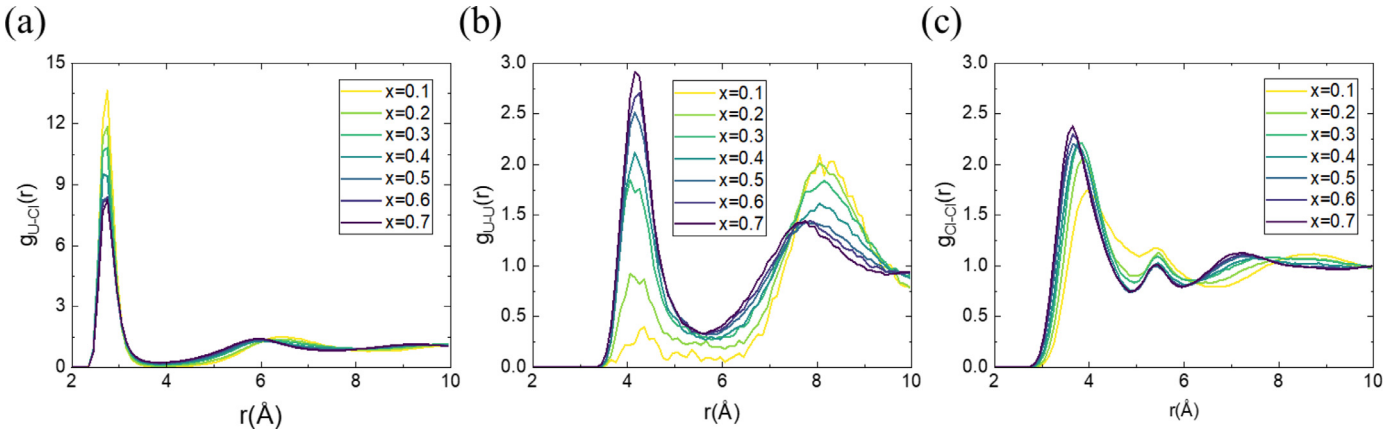

Fig. 2. The radial distribution functions of (a) U-Cl, (b) U-U and (c) Cl-Cl as a function of U concentration at 800 °C.

the eutectic composition, the viscosity decreases by 64.21% from 5.84 cP to 2.09 cP under identical temperature increases, resulting in notably higher temperature dependence. Similarly, the contour lines in Fig. 1c exhibit an approximately 45° slope with increasing UCl_3 content.

The RDFs of the computed molten salt mixtures at 800 °C provide molecular-level insights into the fluidic properties (Fig. 2). The RDFs between U and Cl show identical nearest-neighbor peak positions among all compositions considered (Fig. 2a), with decreasing heights upon increasing uranium content. The second peak position in U-Cl RDFs shifts inward from 6.54 Å to 5.93 Å, as the UCl_3 content increases from 10 mol% to 70 mol%, showing more tightly bound solvation shells with increasing U contents. It is noted that the local minimum between the first and second peaks increases with increasing U content. The RDFs between U and U also exhibit identical nearest-neighbor peaks, yet the peak height increases with the UCl_3 contents (Fig. 2b). The second peak heights in U-U RDFs show decreasing peak height as well as bond lengths with increasing U-Cl peak height. These results show that uranium becomes closer to each other with increasing UCl_3 content, in such a manner that U^{3+} ions may overlap their first solvation shell. The Cl-Cl RDFs show less dramatic change upon composition change, yet with clear trends of decreasing nearest neighbor Cl-Cl bond lengths and increasing peak heights (Fig. 2c).

The coordination and local environment analyses show the formation of U network structures inside the molten salt. The cutoffs for the coordination analyses are determined from local minimum points (4.0 Å) in the RDF analyses in Fig. 2a. Fig. 3a shows that 7- and 8-fold coordination among U^{3+} ions increases while 5- and 6-fold coordination decrease with respect to increasing UCl_3 contents. The RDF analyses in Figs. 2a and 2b reveal that U^{3+} ions get coordinated increasingly by other U^{3+} ions since U-Cl bonds decrease in relative amount with respect to the UCl_3 content. The fraction of U that gets coordinated by one or more U^{3+} is counted in terms of the total number of U that participates in the network in Fig. 3b. At 10 mol% UCl_3, almost all UCl_3 exists in the monomer form. As the U content increases, the fraction for U monomer sharply decreases, initially forming U_2Cl_6 dimer at 20 mol% UCl_3, then forming mostly $U_mCl_n^{-(n-3m)}$ ($m>4$) polymer inside the molten salt. Near the eutectic composition of 53 mol% UCl_3, almost all U^{3+} exists in polymer form. At 30 mol%, the fraction of U polymer decreases from 37% to 26% from 600 °C to 800 °C, showing that thermal energy breaks down the polymer formation (Fig. 3c). In the identical temperature range, however, the polymer fraction of U does not change for the eutectic and higher compositions (Fig. 3d).

The nature of bonding among uranium polyhedra also changes upon composition change (Fig. 3e). At 10 mol%, uranium polyhedra consisting of U^{3+} coordinated by Cl^- are largely connected by sharing polyhedral corners or equivalently one Cl^- ion. As the U content increases, corner-sharing sharply decreases while increasing the fraction of edge-sharing (sharing 2 Cl^- ions) and face-sharing (sharing 3 Cl^- ions) polyhedra. At 70 mol%, the fraction of edge-sharing polyhedra reaches 45%, followed by a nearly identical fraction of corner-sharing (27%) and face-sharing polyhedra (27%). Also, the kinetic barrier for configuration changes, computed from the RDFs of U-Cl, decreases with increasing UCl_3 content. Kinetic

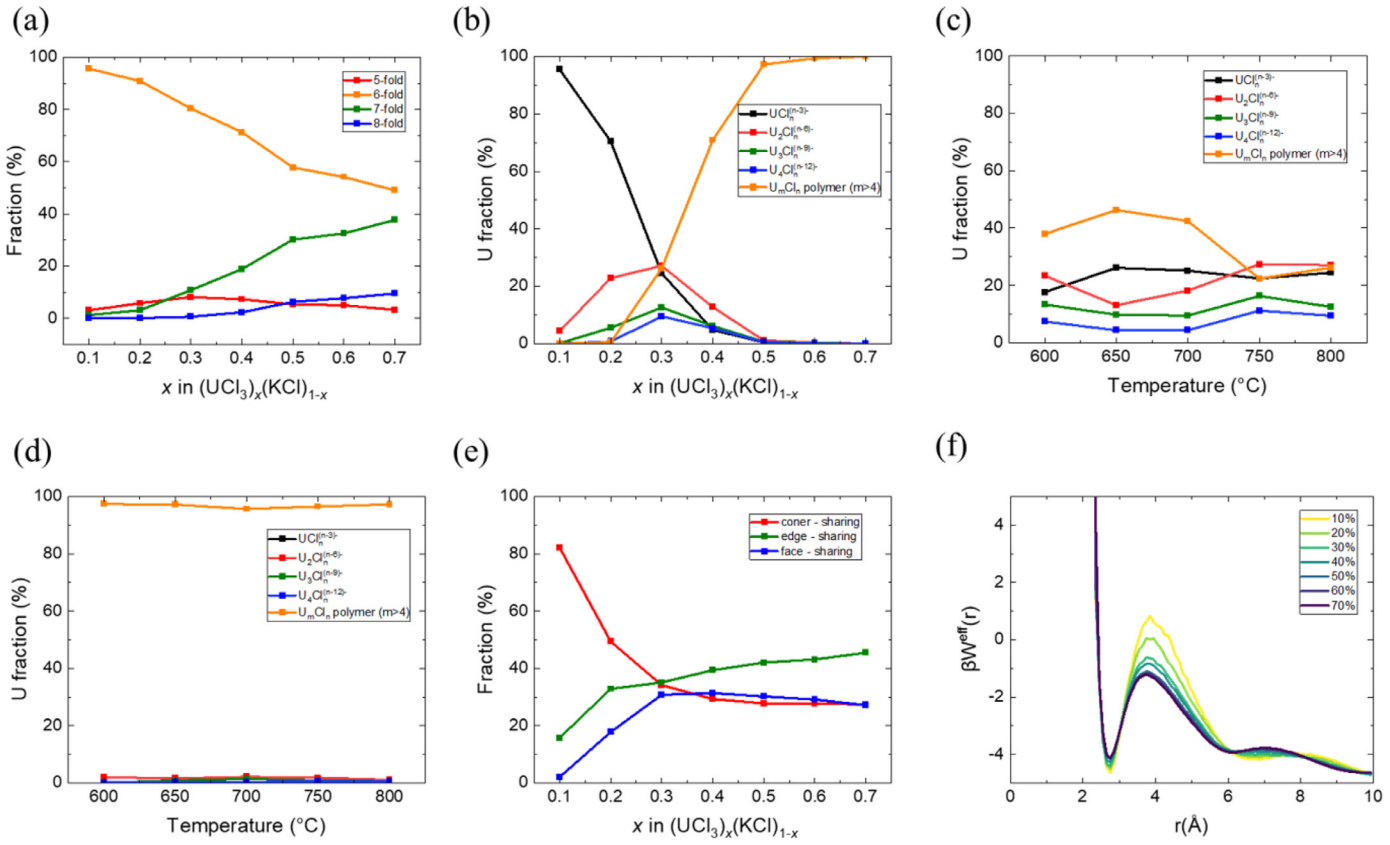

Fig. 3. Ionic local structure analyses. (a) The coordination environment of U3+ ions inside the molten salt according to the composition (b) The fraction of UCl3 monomers/oligomers and polymer-like network structures of KCl-UCl3 at various uranium concentration at 800 °C (c) The fraction of UCl_3 monomers and oligomers/polymers of KCl-30%UCl_3 according to temperature (d) The fraction of UCl_3 monomers and oligomers/polymers of KCl-50%UCl_3 according to temperature (e) The fraction of corner-, edge- and face-sharing polyhedra inside the molten salts at 800 °C according to composition (f) The kinetic barrier estimated based on U-Cl RDFs according to composition.

barrier heights are derived by the equation below:

$$\beta W_{ij}^{eff}(r) = -\ln g_{ij}(r) - 2\ln(r)$$

where $g_{ij}(r)$ represents the U-Cl partial radial distribution functions [33]. Compared to KCl-10% UCl_3, the barrier height decreases by 44.12% at 50 mol% and 46.48% at 70 mol% UCl_3 composition (Fig. 3f).

The heat-transfer performances of molten salts during forced and natural convection are evaluated using the Fig. of demerits (FOD), based on ratio between the rate of heat transfer and the pumping power by Bonilla [34]

$$\text{FOD (forced convection, turbulent)} = \mu^{0.2}/\rho^2 C_p^{2.8}$$

$$\text{FOD (natural convection, turbulent)} = \left[\mu^{0.2}/\beta\rho^2 C_p^{1.8}\right]^{0.36}$$

where μ, ρ, C_p and β indicate viscosity, density, heat capacity, and volume expansivity, respectively. The FOD of forced convection is based on minimal pumping power for a given coolant temperature rise. Increased FOD of forced convection refers to demanding more pumping power to run the fluids. FOD of natural turbulent convection bases more on the heat removal performance. Increased FOD of natural convection indicates that larger temperature change of fluid is needed to transfer heat. This may result in lowered safety and efficiency of the reactors. The plotted FODs for both forced turbulent and natural turbulent convection show little dependency on temperature while increasing uranium content, in general, raises the FOD values (Fig. 4). The natural turbulent convection FOD interestingly exhibits a local minimum near the eutectic composition, with a local maximum near 30 mol% compositions. The computed FODs also show that increasing U content beyond 60% results in a rapid increase of the FOD.

Discussion

The computed densities are overall underestimated compared to experimental values and deviate from approximately 5 to 20%. The largest error occurred at KCl-53% UCl_3 composition at 700 °C, where the computed value is 3.16 g/cm^3 while the experimentally measured data was 19.5% higher at 3.92 g/cm^3 [7]. At another eutectic composition of KCl-20% UCl_3, the computed density decreases from 2.25 g/cm^3 to 2.11 g/cm^3, as the temperature increases from 600 °C to 800 °C, while the experimental density decreases from 2.53 g/cm^3 to 2.30 g/cm^3 [7].

The difference between the calculated density and the reference experimental data appears larger than the other simulations. The interatomic potentials employed in this study were applied in several previous reports to calculate the properties of uranic molten salts [17,19,35]. The errors in the calculated values in this study may be caused by the difference in the model system from the original model system used to obtain the potential parameters. Within this study, however, investigating the tendency of thermal properties changes depending on the concentration and temperature.

Viscosities of KCl-UCl_3 molten salts are rarely reported in the literature, with the only available data for fused KCl-UCl_3-UCl_4 (79.9% UCl_3 + 20.1% UCl_4) systems. Compared to this system, the PIM model overestimates the viscosities for KCl-UCl_3 by approximately 5~65%, except for the KCl-10%UCl_3. At the eutectic concentration of KCl-53%UCl_3, the computed viscosity decreases from 5.83

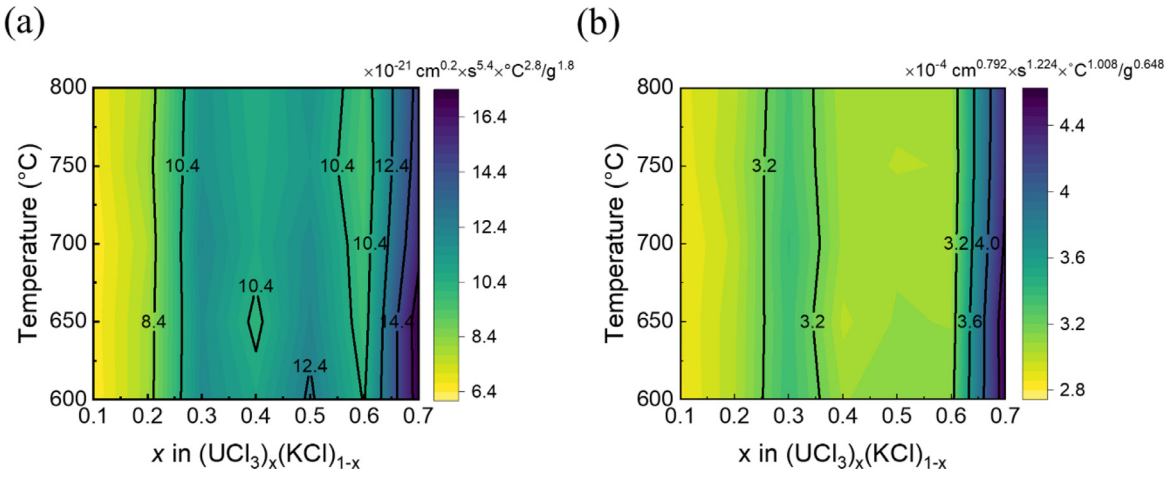

Fig. 4. The figure of demerit computed for (a) forced turbulent convection and (b) natural turbulent convection according to temperature and composition.

cP to 2.01 cP, as the temperature increases from 600 °C to 800 °C, while experimentally measured viscosity decreases from 3.52 cP to 1.71 cP in the same temperature range [9]. Interestingly, the degree of viscosity overestimation is significantly less with KCl-UCl_3 molten salts compared to that of NaCl-UCl_3 [8], despite employing identical interatomic potential models. We could not find any experimental reference on the heat capacities of KCl-UCl_3 molten salts.

Among the molten salt properties, it is noted that temperature dependence largely arises only among viscosities, while the densities and heat capacities exhibit weak dependency on temperature. While low U content KCl-UCl_3 exhibits a coefficient of thermal expansion similar to that of water, increasing U content reduces the coefficient of thermal expansion, possibly due to the formation of U network structures. Viscosities, however, exhibit the opposite behavior with respect to temperature; increasing U content lowers the slopes for the contour map and increases the temperature dependence, especially near the eutectic composition.

This temperature dependence is counterintuitive at first, especially with the temperature-independent fraction of U participating in the network structure. The U network structure, identified by the shared first solvation shell among U-Cl polyhedra, exhibits tightly bound, yet shared Cl- ions among U^{3+} ions and thus increases the molten salts' viscosity. In our calculations, the relative amount of U network structure does not change in the temperature range considered, suggesting that the viscosity decrease with increasing temperature is not solely caused by the thermal breakup of the U network structures near the eutectic temperature. One possible explanation involves the higher kinetic energy of the ions for switching local environment upon increasing U content. The similar amount of corner-, edge- and face-sharing polyhedra in the molten salt, along with higher kinetic energy suggests that the U network structure becomes more flexible, with capabilities to modify the local configurations upon temperature increase [36]. It should be noted that viscosity rarely correlates to lowered kinetic barrier between U and Cl ions at high concentration of UCl_3, which is rather attributed to the increment of shared Cl^- ions as large chuck of the U network gets developed. Another explanation involves the increase in free volume inside the molten salt with increasing temperature. Since the amount of U network structure remains constant despite the thermal expansion, the thermal expansion largely increases the amount of free volume, possibly lowering the viscosities with temperature.

Based on the equations for the FOD for molten salts, one easily deduces that density and heat capacity largely dominate the forced convection and natural convection. In this sense, the temperature insensitivity of the FODs is understood; both heat capacity and density get affected little by temperature in the range that we considered. Also, the fluctuation in forced convection FOD from 30 mol% to 60 mol% is understood from the small fluctuations in the computed heat capacity shown in Fig. 2b. Since the forced convection FOD translates to the pumping power needed to create flow, low U content may be beneficial for forced convection. Yet, similar FOD values among 30~60 mol% U content lead to the eutectic point as the preferable composition for forced convection, given that high U loading may allow long cycle duration in the reactor operation. The temperature insensitivity of the FOD also makes it easy to design the pumps in the operating temperature range. Under natural convection scenario, the molten salt exhibit similar tendency with the forced convection, where the composition rather than temperature dominates the salt properties. At 53 mol% UCl_3 eutectic composition, the salt exhibits lower FOD than the nearby compositions. This trend encourages designing the molten salt reactors with the molten salt at the eutectic composition.

Table 2
The computed molar volume according to the temperature.

Temperature (°C)	600	650	700	750	800
V_m (Å^3/mol)	141.54	144.93	145.32	147.66	148.77

Conclusions

In this work, we investigate the physicochemical properties of KCl-UCl_3 molten salts according to uranium concentration and temperature. The molten salt system exhibits a high UCl_3 composition of 53% at the eutectic mixture, and local environment analyses reveal that U^{3+} exists in polymer-like network structures, sharing Cl^- ions among two or more U^{3+} ions. The polymer-like network structures within the molten salts demonstrate uniquely high, yet temperature-dependent viscosity values, providing the molten salt system's potential for natural circulation. These features call for further detailed investigation of this interesting molten salt system in terms of fluid dynamic properties such as thermal conductivity and dimensionless Prandtl number, to properly assess the molten salt system's capability in natural circulation. Table 2

Declaration of Competing Interest

The authors declare that they have no known competing financial interests or personal relationships that could have appeared to influence the work reported in this paper.

CRediT authorship contribution statement

Hyeonwoo Kim: Data curation, Methodology, Investigation, Writing – original draft. **Choah Kwon:** Conceptualization, Methodology, Software, Formal analysis, Writing – original draft. **Seongwon Ham:** Investigation. **Juhyung Lee:** Investigation. **Sung Joong Kim:** Funding acquisition, Project administration. **Sangtae Kim:** Conceptualization, Writing – review & editing.

Data Availability

Data will be made available on request.

Acknowledgment

This work is supported by the National Research Foundation of Korea (NRF), funded by the Ministry of Science and ICT, the Republic of Korea (No. NRF-2021M2D2A2076378) H. Kim and S. Kim acknowledge the support from the Human Resources Development program (no. 20204010600090) of the Korea Institute of Energy Technology Evaluation and Planning (KETEP), funded by the Ministry of Trade, Industry, and Energy of the Korean Government. This work was also supported by the research fund of Hanyang University under the grant number HY-202100000670017.

Supplementary materials

Supplementary material associated with this article can be found, in the online version, at doi:10.1016/j.jnucmat.2023.154329.

References

[1] G. Locatelli, M. Mancini, N. Todeschini, Generation IV nuclear reactors: current status and future prospects, Energy Policy 61 (2013) 1503–1520, doi:10.1016/j.enpol.2013.06.101.
[2] J.C. Gehin, D.E. Holcomb, G.F. Flanagan, B.W. Patton, R.L. Howard, T.J. Harrison, Fast Spectrum Molten Salt Reactor Options, 2011. https://doi.org/10.2172/1018987.
[3] C.W. Forsberg, Hydrogen Production Using the Advanced High-Temperature Reactor, (n.d.) 13.
[4] T. SCHÖNFELDT, J.S. NIELSEN, E.E. PETTERSEN, A.V. PEDERSEN, D.J. COOPER, Molten salt reactor, EP3639279A1, 2020. https://patents.google.com/patent/EP3639279A1/en?q=seaborg+reactor&oq=seaborg+reactor (accessed August 5, 2022).
[5] A.T.C. JR, K. Czerwinski, B.S. EL-DASHER, W.M. Kerlin, K. Kramer, J.F. Latkowski, R.C. Petroski, J.C. Walter, Molten nuclear fuel salts and related systems and methods, US20160189813A1, 2016. https://patents.google.com/patent/US20160189813A1/en?q=molten+chloride+fast+reactor&assignee=terrapower&oq=terrapower+molten+chloride+fast+reactor (accessed August 5, 2022).
[6] J.H. Park, W. Choi, J. Lim, T. Kim, Y. Kim, Y. Yoon, S. Kim, S.J. Kim, Design Concepts and Requirements of Passive Molten Salt Fast Reactor (PMFR) (2022) 6.
[7] G.J. Janz, R.P.T. Tomkins, C.B. Allen, J.R. Downey, G.L. Garner, U. Krebs, S.K. Singer, Molten salts: volume 4, part 2, chlorides and mixtures—Electrical conductance, density, viscosity, and surface tension data, J. Phys. Chem. Ref. Data. 4 (1975) 871–1178, doi:10.1063/1.555527.
[8] V.N. Desyatnik, S.F. Katyshev, S.P. Raspopin, Yu.F. Chervinskii, Density, surface tension, and viscosity of uranium trichloride-sodium chloride melts, Sov. At. Energy. 39 (1975) 649–651, doi:10.1007/BF01121527.
[9] S.F. Katyshev, Yu.F. Chervinskii, V.N. Desyatnik, Density and viscosity of fused mixtures of uranium chlorides and potassium chloride, Sov. At. Energy. 53 (1982) 565–566, doi:10.1007/BF01122100.
[10] L.C. Dewan, C. Simon, P.A. Madden, L.W. Hobbs, M. Salanne, Molecular dynamics simulation of the thermodynamic and transport properties of the molten salt fast reactor fuel LiF–ThF4, J. Nucl. Mater. 434 (2013) 322–327, doi:10.1016/j.jnucmat.2012.12.006.
[11] J.-.B. Liu, X. Chen, Y.-.H. Qiu, C.-.F. Xu, W.H.E. Schwarz, J. Li, Theoretical Studies of Structure and Dynamics of Molten Salts: the LiF–ThF4 System, J. Phys. Chem. B. 118 (2014) 13954–13962, doi:10.1021/jp509425p.
[12] B. Li, S. Dai, D. Jiang, First-Principles Molecular Dynamics Simulations of UCln–NaCl (n = 3, 4) Molten Salts, ACS Appl. Energy Mater. 2 (2019) 2122–2128, doi:10.1021/acsaem.8b02157.
[13] A. Aguado, L. Bernasconi, S. Jahn, P.A. Madden, Multipoles and interaction potentials in ionic materials from planewave-DFT calculations, Faraday Discuss 124 (2003) 171–184, doi:10.1039/B300319C.
[14] M. Salanne, B. Rotenberg, S. Jahn, R. Vuilleumier, C. Simon, P.A. Madden, Including many-body effects in models for ionic liquids, Theor. Chem. Acc. 131 (2012) 1143, doi:10.1007/s00214-012-1143-9.
[15] B. Li, S. Dai, D. Jiang, Molecular dynamics simulations of structural and transport properties of molten NaCl-UCl3 using the polarizable-ion model, J. Mol. Liq. 299 (2020) 112184, doi:10.1016/j.molliq.2019.112184.
[16] T. Jiang, N. Wang, S. Peng, L. Yan, Structural and transport characteristics of UCl3 in molten LiCl-KCl mixture: a molecular dynamics simulation study, Chem. Res. Chin. Univ. 31 (2015) 281–287, doi:10.1007/s40242-015-4331-z.
[17] J.-.X. Dai, W. Zhang, C.-.L. Ren, H. Han, X.-.J. Guo, Q.-.N. Li, Molecular dynamics investigation on the local structures and transport properties of uranium ion in LiCl-KCl molten salt, J. Nucl. Mater. 511 (2018) 75–82, doi:10.1016/j.jnucmat.2018.08.052.
[18] X. Li, J. Song, S. Shi, L. Yan, Z. Zhang, T. Jiang, S. Peng, Dynamic Fluctuation of U3+ Coordination Structure in the Molten LiCl–KCl Eutectic via First Principles Molecular Dynamics Simulations, J. Phys. Chem. A. 121 (2017) 571–578, doi:10.1021/acs.jpca.6b10193.
[19] G.I.L. van Oudenaren, J.A. Ocadiz-Flores, A.L. Smith, Coupled structural-thermodynamic modelling of the molten salt system NaCl-UCl3, J. Mol. Liq. 342 (2021) 117470, doi:10.1016/j.molliq.2021.117470.
[20] D.A. Andersson, B.W. Beeler, Ab initio molecular dynamics (AIMD) simulations of NaCl, UCl3 and NaCl-UCl3 molten salts, J. Nucl. Mater. 568 (2022) 153836, doi:10.1016/j.jnucmat.2022.153836.
[21] L. Rycerz, J. Kapala, M. Gaune-Escard, Experimental mixing enthalpy and thermodynamic modelling of UCl3-KCl system, J. Mol. Liq. 342 (2021) 116963, doi:10.1016/j.molliq.2021.116963.
[22] M. Salanne, C. Simon, P. Turq, P.A. Madden, Calculation of Activities of Ions in Molten Salts with Potential Application to the Pyroprocessing of Nuclear Waste, J. Phys. Chem. B. 112 (2008) 1177–1183, doi:10.1021/jp075299n.
[23] T.D. Kühne, M. Iannuzzi, M. Del Ben, V.V. Rybkin, P. Seewald, F. Stein, T. Laino, R.Z. Khaliullin, O. Schütt, F. Schiffmann, D. Golze, J. Wilhelm, S. Chulkov, M.H. Bani-Hashemian, V. Weber, U. Borštnik, M. Taillefumier, A.S. Jakobovits, A. Lazzaro, H. Pabst, T. Müller, R. Schade, M. Guidon, S. Andermatt, N. Holmberg, G.K. Schenter, A. Hehn, A. Bussy, F. Belleflamme, G. Tabacchi, A. Glöß, M. Lass, I. Bethune, C.J. Mundy, C. Plessl, M. Watkins, J. VandeVondele, M. Krack, J. Hutter, CP2K: an electronic structure and molecular dynamics software package - Quickstep: efficient and accurate electronic structure calculations, J. Chem. Phys. 152 (2020) 194103, doi:10.1063/5.0007045.
[24] Y. Okamoto, P.A. Madden, K. Minato, X-ray diffraction and molecular dynamics simulation studies of molten uranium chloride, J. Nucl. Mater. 344 (2005) 109–114, doi:10.1016/j.jnucmat.2005.04.026.
[25] F. HUTCHINSON, M. WILSON, P.A. MADDEN, A unified description of MCl3 systems with a polarizable ion simulation model, Mol. Phys. 99 (2001) 811–824, doi:10.1080/00268970010022878.
[26] W.J. Glover, P.A. Madden, Raman spectra of ionic liquids: a simulation study of LaCl3 and its mixtures with alkali chlorides, J. Chem. Phys. 121 (2004) 7293–7303, doi:10.1063/1.1792574.
[27] S. Wang, S. Xiao, W. Hu, H. Deng, Effect of MCl3 (M=La, U or *Sc*) component on the local structures and transport properties of LiCl–KCl–MCl3 eutectic: a molecular dynamics study, Electrochim. Acta 306 (2019) 366–376, doi:10.1016/j.electacta.2019.03.123.
[28] Malcolm W. Chase National Information Standards Organization (US), NIST-JANAF Thermochemical Tables, 9, American Chemical Society, Washington, DC, 1998.
[29] Y. Zhang, A. Otani, E.J. Maginn, Reliable Viscosity Calculation from Equilibrium Molecular Dynamics Simulations: a Time Decomposition Method, J. Chem. Theory Comput. 11 (2015) 3537–3546, doi:10.1021/acs.jctc.5b00351.
[30] B. Hess, Determining the shear viscosity of model liquids from molecular dynamics simulations, J. Chem. Phys. 116 (2002) 209, doi:10.1063/1.1421362.
[31] O. Borodin, G.D. Smith, Structure and Dynamics of *N* -Methyl- *N* -propylpyrrolidinium Bis(trifluoromethanesulfonyl)imide Ionic Liquid from Molecular Dynamics Simulations, J. Phys. Chem. B. 110 (2006) 11481–11490, doi:10.1021/jp061593o.
[32] J. Schorne-Pinto, J.A. Yingling, M.S. Christian, A.M. Mofrad, M.A.A. Aslani, T.M. Besmann, Correlational Approach to Predict the Enthalpy of Mixing for Chloride Melt Systems, ACS Omega 7 (2022) 362–371, doi:10.1021/acsomega.1c04755.
[33] M. Levesque, V. Sarou-Kanian, M. Salanne, M. Gobet, H. Groult, C. Bessada, P.A. Madden, A.-.L. Rollet, Structure and dynamics in yttrium-based molten rare earth alkali fluorides, J. Chem. Phys. 138 (2013) 184503, doi:10.1063/1.4802986.
[34] C.F. Bonilla, H. Etherington, Comparison of Coolants, McGraw-Hill, 1958.
[35] Y. Yang, J. Lan, B. Liang, D. Wang, L. Chen, M. Zhang, C. Jiao, G. Wang, R. Geldiyev, Y. Li, Z. Zheng, Y. Sun, W. Zhou, W. Shi, Molecular Dynamics Simulations of Metal Electrode/Molten LiCl-KCl-UCl$\less$sub$\greater$3$\less$/sub$\greater$ Mixtures Interface, J. Electrochem. Soc. 169 (2022) 032503, doi:10.1149/1945-7111/ac579a.
[36] D. Corradini, P.A. Madden, M. Salanne, Coordination numbers and physical properties in molten salts and their mixtures, Faraday Discuss 190 (2016) 471–486, doi:10.1039/C5FD00223K.